

${}^5_{\Xi}H$ hypernuclei by folding the state-of-the-art ΞN interactions

Faisal Etminan*

*Department of Physics, Faculty of Sciences,
University of Birjand, Birjand 97175-615, Iran and
Interdisciplinary Theoretical and Mathematical Sciences
Program (iTHEMS), RIKEN, Wako 351-0198, Japan*

(Dated: June 7, 2024)

I examined a phenomenological Nijmegen and a first principles HAL QCD ΞN potentials to study $\alpha\Xi$ interactions. A Woods-Saxon type form for $\alpha\Xi$ potential in the single-folding potential approach is derived by using the spin- and isospin averaged ΞN interactions. The possibility of resonance or bound state is searched and accordingly, the low energy scattering phase shift parameters of $\alpha\Xi$ are calculated. The numerical results show that even though two ΞN potentials have significantly dissimilar isospin (I) and spin (S) components, ${}^5_{\Xi}H$ could be only a Coulomb-assisted resonance state that appears about 0.5 MeV below the threshold of $\alpha + \Xi^-$ for both model of potentials.

I. INTRODUCTION

Although there is a lot of interest in knowing about hyperon interactions, the underlying ΞN interaction is facing many uncertainties. The main reason is the lack of experimental data. In this regard, many researches have been conducted recently, both experimentally and theoretically, such as high resolution gamma-ray experiments [1], KISO event [2], femtoscopic measurements of pp, pA and AA collisions in the ALICE and STAR experiments [3], femtoscopic study of ΞN correlation function in heavy-ion collisions [4, 5] and advanced few-body theoretical methods [6–15], Jacobi no-core shell model (J-NCSM) [16] and lattice QCD calculations [17, 18].

Hiyama et al. in Ref. [8] studied ${}^5_{\Xi}H$ hypernuclei by using two types of ΞN interactions, the Nijmegen Hard-Core model D (ND) [19] and the Extended Soft-Core model (ESC04)

* fetminan@birjand.ac.ir

[20], it was found to be a Coulomb-assisted bound state, in other words, no nuclear-bound state appeared. While the existence of bound Ξ states in systems with $A = 4 - 7$ baryons based on the chiral ΞN interactions are investigated in Ref. [16] and a clearly bound state about 2.16 ± 0.1 MeV is reported for $\alpha\Xi \left[\frac{5}{\Xi}H \left(J^\pi = \frac{1}{2}^+, T = \frac{1}{2} \right) \right]$. Also, Friedman and Gal [21] by utilizing an optical potential concluded same result for binding energy of $\frac{5}{\Xi}H$ that was 2.0 MeV. Furthermore, Myint and Akaishi [6] by using Nijmegen model-D potential [19] reported 1.7 MeV for binding energy of this system, where authors emphasized that the large part binding energy is due to $\alpha + \Xi^-$ Coulomb interaction.

The $NN\Xi$ and $NNN\Xi$ system studied in Ref. [11] by employing two modern ΞN interactions: a phenomenological Nijmegen ΞN potential (ESC08c) that is established on the meson exchanges [22] and HAL QCD ΞN potential (HAL QCD) which is based on first principle lattice QCD simulations [18]. In Ref. [11] systems with more particles have not been investigated. Therefore, by considering the above results it is necessary to study $\frac{5}{\Xi}H$ by using both state-of-the-art ESC08c and HAL QCD ΞN potential where the latter is the most consistent potentials with the LHC ALICE data [23, 24]. Recently, the HAL QCD Collaboration published the first lattice QCD simulations of the ΞN potential [18]. The simulation was performed by $(2 + 1)$ -flavor with quark masses near the physical point $m_\pi \simeq 146.4$ MeV and $m_K \simeq 525$ MeV on a large lattice space- time volume $\simeq (8.1 \text{ fm})^4$. In addition, the dibaryons systems with multiple strangeness such as $\Lambda\Lambda$, ΞN [18], ΩN [25, 26] and $\Omega\Omega$ [27] have been calculated by HAL QCD method [28–30].

In this work, a Woods-Saxon type form for $\alpha + \Xi$ system is obtained by using single-folding potential (SFP) method. Since the α -cluster has low compressibility property, in this model it is supposed that both particles Ξ and α move in an effective $\alpha\Xi$ potential. The effective $\alpha + \Xi$ nuclear potential is approximated by the single-folding of nucleon density in the α -particle and spin- and isospin averaged ΞN potential between Ξ and a nucleon [6, 31–33].

After that, the resultant $\alpha\Xi$ potential is fitted to a continuous analytical Woods-Saxon type function. Then the Schrödinger equation is solved in the infinite volume by using this fitted function as input to obtain binding energy and relevant scattering observables from the asymptotic behavior of the wave function.

It should be noted here that the SFP models reduced a five-body problem to an effective two-body problem, this can be computational advantage but this approximation may miss some part of the physics of the problem, e.g. the obtained potential might be underestimated.

So to treat this issue as much as possible, here the SFP method is benchmarked and tuned by employing ESC08c ΞN potential only in 3S_1 ($I = 0$) [22] channel as input to reproduce the parameters of common phenomenological Dover-Gal (DG) $\alpha\Xi$ potential [33, 34]. And, this model is accurate just for the low energy features of the $\alpha + \Xi$ system, because it is extracted from the low energy ΞN interactions. There are enormous applications of $\alpha\Xi$ potential in few-body methods based on α -cluster models such as 3-, 4- and 5-body Gaussian expansion [10], J-NCSM [16] and Faddeev [12, 35–37].

The paper is organized as follows. In Sec. II, I provide approximately reliable expressions for the effective ΞN interactions that is defined by averaging on the spin- and isospin components for both ESC08c and HAL QCD ΞN potentials. Also, the single-folding potential approach is described briefly. In Sec. III, the numerical results and discussions are presented. The summary and final conclusions are given in Sec. IV.

II. ΞN INTERACTIONS AND SINGLE-FOLDING POTENTIAL APPROACH

Here, the ESC08c and the HAL QCD ΞN potentials that are used to found effective potentials of $\alpha + \Xi$ systems are described. And a brief description of the SFP model [31, 33] is given.

The ESC08c Nijmegen ΞN potential function consists of local central Yukawa-type potentials with attractive and repulsive terms [12, 22],

$$V_{\Xi N}^{ESC08c}(r) = -A \frac{\exp(-\mu_A r)}{r} + B \frac{\exp(-\mu_B r)}{r}. \quad (1)$$

where the low-energy data and the parameters of these models are given in Table I of Ref. [12].

For ΞN HAL QCD potential, the concrete parametrizations, are taken straight from Ref. [18] at the imaginary-time slices $t/a = 11, 12, 13$ where $a = 0.0846$ fm is the lattice spacing. Sasaki et al. in Ref. [18] clearly treated $\Lambda\Lambda - \Xi N$ interactions by the HAL QCD coupled-channel formalism [30, 38]. The S-wave ΞN interactions is classified in four channels ${}^{11}S_0, {}^{31}S_0, {}^{13}S_1$ and ${}^{33}S_1$. Here same as Ref. [18] the spectroscopic notation ${}^{2I+1, 2S+1}S_J$ is employed where I, S and J indicate the total isospin, the total spin, and the total angular momentum, respectively.

For phenomenological applications, the lattice QCD potential was fitted by analytic func-

tional forms composed of multiple Gaussian and Yukawa functions. The Gauss functions set out the short range part of the potential and Yukawa functions describe the meson exchange picture at medium to long range distances

$$V_{\Xi N}(r) = \sum_{i=1}^3 \alpha_i e^{-r^2/\beta_i^2} + \lambda_2 [\mathcal{Y}(\rho_2, m_\pi, r)]^2 + \lambda_1 \mathcal{Y}(\rho_1, m_\pi, r), \quad (2)$$

where the values of the parameters $\alpha_{1,2,3}, \beta_{1,2,3}, \lambda_{1,2}$ and $\rho_{1,2}$ are given in Table 4 of Ref [18]. $m_\pi \simeq 146$ MeV is the pion mass that was measured on the lattice. I have also presented results by considering the physical value of the pion mass $m_\pi \simeq 138$ MeV. The form factor \mathcal{Y} defines Yukawa function

$$\mathcal{Y}(\rho, m, r) \equiv \left(1 - e^{-\frac{r^2}{\rho^2}}\right) \frac{e^{-mr}}{r}. \quad (3)$$

Since the $\alpha\Xi^- (\frac{5}{2}^-H)$ system required to show a clear core- Ξ structure, I employ approximately reliable expressions for spin and isospin dependence of ΞN interaction to s -shell (the core nucleons and the Ξ are in S-wave states). Therefore in these approximation, the effective ΞN interactions can be obtained by averaging on the spin- and isospin components [8, 16]

$$\bar{V}_{\Xi N} \simeq \frac{\left(V_{\Xi N}^{11S_0} + 3V_{\Xi N}^{31S_0} + 3V_{\Xi N}^{13S_1} + 9V_{\Xi N}^{33S_1}\right)}{16}. \quad (4)$$

In Fig. 1, I compare ΞN potential for (a) the ESC08c model and (b) the HAL QCD at $t/a = 12$ [18]. The statistical errors are not shown in Fig. 1(b), but are considered in my calculations. Fig. 1 reveals qualitative difference between (a) and (b). Therefore it is interesting to find out how these differences are embodied in the low energy properties of $\frac{5}{2}^-H$.

The effective $\alpha + \Xi$ nuclear potential is approximated by the single-folding of nucleon density $\rho(r')$ in the α -particle and spin- and isospin averaged ΞN potential, $\bar{V}_{\Xi N}(|\mathbf{r} - \mathbf{r}'|)$ between the Ξ particle at \mathbf{r}' and the nucleon at \mathbf{r} [31–33]. The $\alpha\Xi$ potential is defined as

$$V_{\alpha\Xi}(r) = \int \rho(r') \bar{V}_{\Xi N}(|\mathbf{r} - \mathbf{r}'|) d\mathbf{r}', \quad (5)$$

where $\rho(r')$ defined the nucleon density function in α -particle at a distance \mathbf{r}' from its center-of-mass, and it can be chosen as follows [39],

$$\rho(r') = 4 \left(\frac{4\beta}{3\pi}\right)^{3/2} \exp\left(-\frac{4}{3}\beta r'^2\right). \quad (6)$$

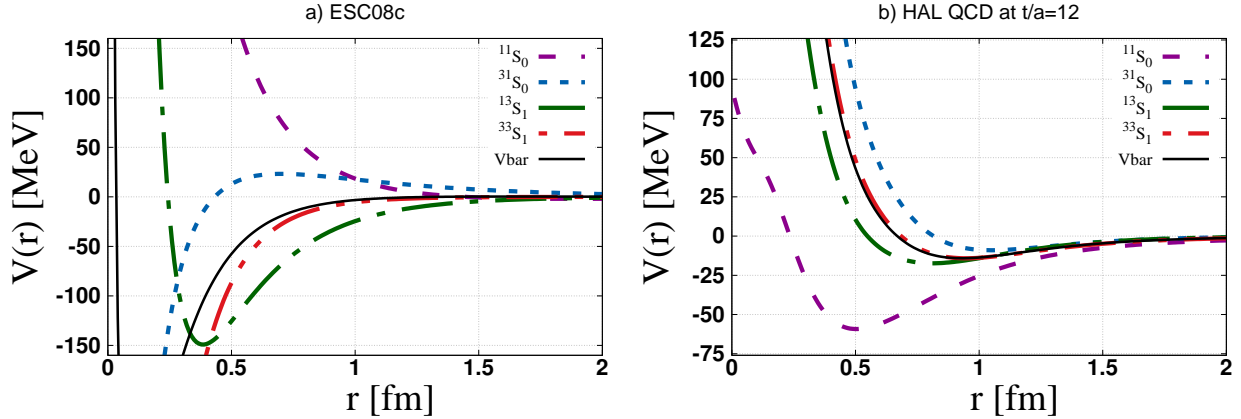


FIG. 1: (a) ESC08c and (b) HAL QCD ($t/a = 12$) ΞN potentials in $^{11}S_0$, $^{31}S_0$, $^{13}S_1$ and $^{33}S_1$ channels. The corresponding scattering phase shifts for each channel are given in Ref. [11]. The solid black line, which is labeled by V_{bar} , shows the spin- and isospin averaged potential, $\bar{V}_{\Xi N}$ in Eq. (1).

The integration in Eq. (5) is over all space as permitted by $\rho(r')$. Normalization conditions require that

$$\int \rho(r') d\mathbf{r}' = 4 \left(\frac{4\beta}{3\pi} \right)^{3/2} \int_0^\infty \exp\left(-\frac{4}{3}\beta r'^2\right) 4\pi r'^2 dr' = 4, \quad (7)$$

here, β is a constant and it could be determined by the rms radius of ^4He [39], $r_{r.m.s} = \frac{3}{\sqrt{8\beta}} = 1.47$ fm.

Finally, a hard-sphere model of Coulomb interaction is employed in my calculations as [37]

$$V_{Coul}(r) = -2\alpha_f \times \begin{cases} \frac{1}{r_{Coul}} \left(\frac{3}{2} - \frac{r^2}{2r_{Coul}^2} \right), & r \leq r_{Coul} \\ \frac{1}{r}, & r > r_{Coul} \end{cases} \quad (8)$$

where α_f is the fine structure constant and $r_{Coul} = 1.47$ fm is the Coulomb radius.

III. NUMERICAL RESULTS

As it has been shown in [8], the $^5_\Xi H$ is not bound with Nijmegen ND and ESC04 ΞN potential, actually it was found to be a Coulomb-assisted bound state. While recently Le et al. [16] reported a clearly bound state about 2.16 ± 0.1 MeV employing a chiral ΞN interactions. In Fig 1, I draw (a) ESC08c and (b) HAL QCD potentials in $^{11}S_0$, $^{31}S_0$, $^{13}S_1$ and $^{33}S_1$ channels and their corresponding spin- isospin averaged potential $\bar{V}_{\Xi N}$. Also, ΞN phase

shifts in each channels relevant to above potentials are drawn and given in Fig. 2 of Ref [11]. It is seen that these two potentials are different. It is therefore desirable to examine the ${}^5_{\Xi}H$ by ESC08c and HAL QCD potentials for the purpose of seeing whether such differences are manifest in the predictions for low energy properties. Since the α particle is strongly bound, the mass gap between ΞN and $\Lambda\Lambda$ is somehow abolished [6] that makes this light hypernucleus to be interesting and to be studied straightforwardly.

$\alpha\Xi$ potential is obtained by solving Eq. (5) and the resultant potentials are depicted in Fig. 2 at the imaginary-time distances $t/a = 11, 12, 13$ for HAL QCD potentials. Also for comparison the ESC08c and the common DG potentials are shown.

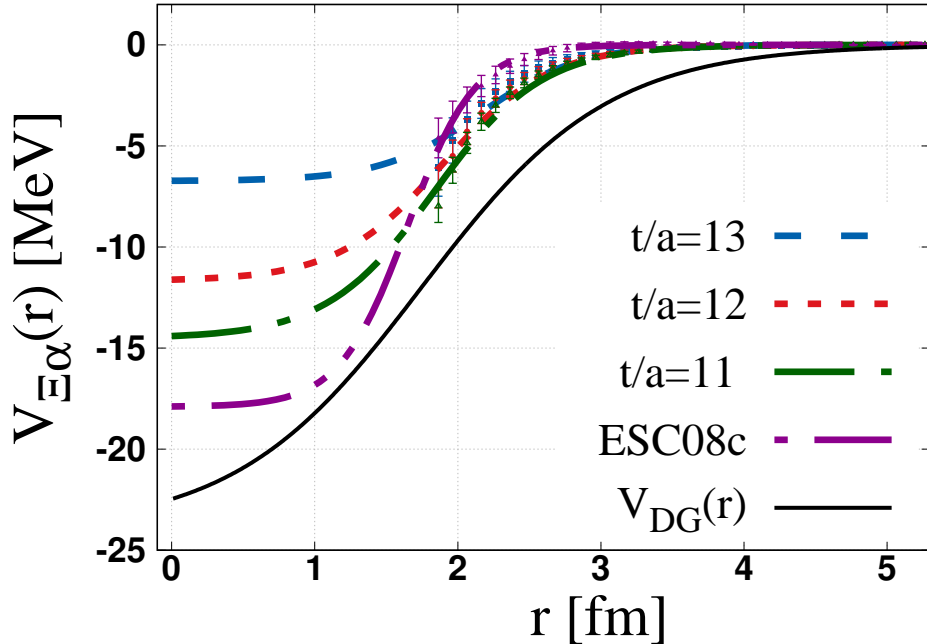


FIG. 2: $V_{\alpha\Xi}(r)$, the single-folding potentials that have been obtained by Eq. (5) using ΞN potential models of DG (solid black line), ESC08c (dash-double-dotted magenta line) and HAL QCD at $t/a = 11$ (dash-dotted green line), $t/a = 12$ (dotted red line) and $t/a = 13$ (dashed blue line). The corresponding ΞN potentials are depicted in Fig. 1.

For phenomenological application and calculation of observables, such as scattering phase shifts and binding energies, I fit $V_{\alpha\Xi}(r)$ to a Wood-Saxon form using the function that given by Eq. (9) (motivated by common DG model of potential [34]) with three parameters, V_0 , R and c ,

$$V_{\alpha\Xi}^{DG}(r) = -V_0 \left[1 + \exp\left(\frac{r-R}{c}\right) \right]^{-1}, \quad (9)$$

where V_0 is known as the depth parameter, $R = 1.1A^{1/3}$ with A being the mass number of the nuclear core, i.e α ($A = 4$) and c is known as the surface diffuseness. By using the fit functions (solid lines in Fig 2) as input the Schrödinger equation were solved in the infinite volume to extract binding energy and scattering observables from the asymptotic behavior of the wave function. Fig. 3 shows $\alpha\Xi$ phase shifts calculated with DG [34], ESC08c and HAL QCD ($t/a = 12$) potentials for comparison. The phase shift in the case of DG potential shows an attractive interaction even to form a bound state with the binding energy about 2 MeV, while attraction in the case of ESC08c is relatively weaker, and for HAL QCD potential is more weak than the previous two cases.

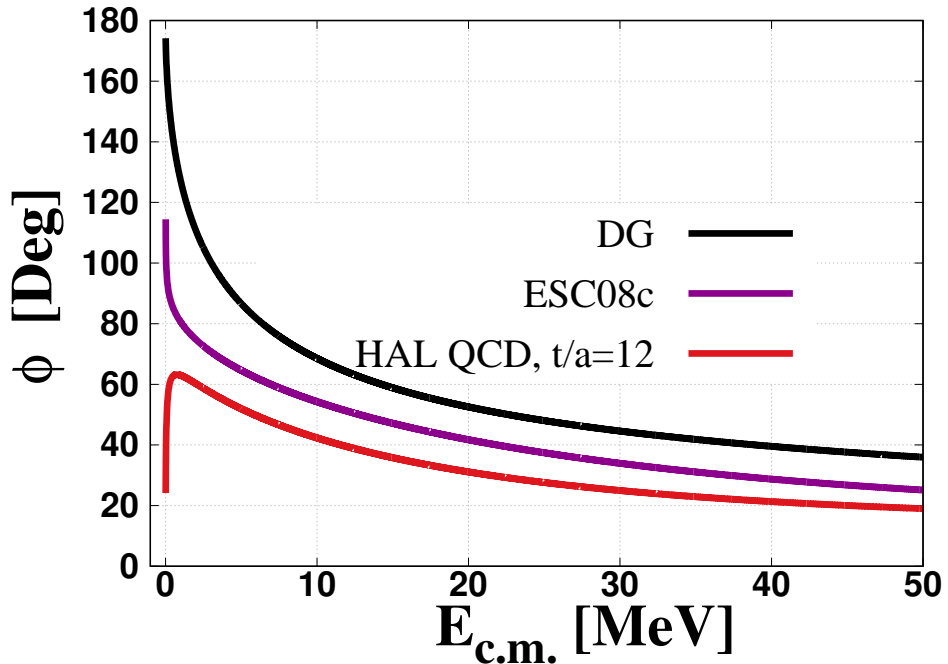


FIG. 3: $\alpha\Xi$ phase shifts using the DG [34], ESC08c and HAL QCD ($t/a = 12$) potentials.

Low-energy part of $\alpha\Xi$ phase shifts in Fig. 3 provides the scattering length (a_0) and the effective range (r_0) by employing the effective range expansion (ERE) formula up to the next-leading-order (NLO),

$$k \cot \delta_0 = -\frac{1}{a_0} + \frac{1}{2}r_0k^2 + \mathcal{O}(k^4). \quad (10)$$

The fit parameters, scattering length, effective range and binding energy $B_{\alpha\Xi^0}$, with DG, ESC08c and HAL QCD potentials are given in Table I. The fit function by these parameters are plotted in Fig. 2 by solid lines. As quoted in the caption of Table I, the numbers

between parenthesis correspond to the calculations by using Ξ mass derived by the lattice simulations [18], where they are slightly bigger than experimental mass. Since by increasing the mass, contribution of repulsive kinetic energy will decrease and finally leads to slightly deeper binding energies. Moreover, binding energies, $B_{\alpha\Xi^-}$ ($B_{\alpha\Xi^0}$), with (without) Coulomb interactions are given. A Coulomb potential due to a uniformly charged sphere of radius r_{Coul} is included, see Eq. (8). If a nuclear-unbound system turn into bound state with support of the attractive Coulomb potential, that is called a Coulomb-assisted bound state. According to behaviour of phase shifts in Fig. 3 and data in Table I none of the ESC08c potential and the HAL QCD potentials ($t/a = 11, 12$ and $t/a = 13$) supports a bound states for ${}^5_{\Xi}H$. Nevertheless, if I switch on the Coulomb interaction, the ${}^5_{\Xi}H$ system become Coulomb-assisted bound state and the corresponding binding energies $B_{\alpha\Xi^-}$ are given in Table I. Definitely as expected, their values are small which is less than 1 MeV. Moreover, when the strong interactions are switched off no bound or resonance states are obtained. So, ${}^5_{\Xi}H$ cannot be a Coulomb-bound (atomic) state.

Based on Hiyama et al.'s numerical results [11], it is expected that the differences in magnitude of binding energies between the ESC08c and HAL QCD potentials should be almost significant, but it is not large here. In addition to the fact that my methods are different, there are two reasons. One reason is that I have used the spin- and isospin averaged potentials here but they did not. Another reason could be that Hiyama et al., in order to treat the coupled-channel effects, they normalized contribution from higher channels $\Xi N - \Lambda\Sigma - \Sigma\Sigma$ in ${}^{33}S_1$ into a $\Xi N - \Xi N$ effective central potential by including a Gaussian function as, $-233 \exp(-r^2)$ [11]. This factor dramatically increases the attractive power of the potential in ESC08 case. I did not inserted this factor in my calculations.

IV. SUMMARY AND CONCLUSIONS

${}^5_{\Xi}H$ hypernuclei is studied by several few-body technics by different ΞN interactions and inconsistent results are reported. Since there are not any sufficient experimental data about Ξ -hypernuclei, the lattice QCD simulation is the most reliable approach. Recently, the HAL QCD Collaboration derived ΞN interaction with quark masses near the physical point $m_\pi \simeq 146.4$ MeV by lattice QCD simulations. Therefore, I examined the ${}^5_{\Xi}H$ by using two significantly different spin- and isospin averaged potentials, i.e phenomenological Nijmegen

TABLE I: The fit parameters of $\alpha\Xi$ potential in Eq. (9) and the corresponding low-energy parameter, scattering length a_0 , effective range r_0 and binding energy $B_{\alpha\Xi^0}$, are given for DG, ESC08c and HAL QCD potentials. Here the NB is an acronym for No Bound or resonance states. The parameter of DG $\alpha\Xi$ potentials are taken directly from Ref. [34].

The results have been achieved by using the experimental masses of α and Ξ , 3727.38 MeV/ c^2 and 1318.07 MeV/ c^2 respectively. Also, the results corresponding to Ξ mass value derived by the HAL QCD Collaboration 1355.2 MeV/ c^2 are given between parenthesis. $B_{\alpha\Xi^-}$ ($B_{\alpha\Xi^0}$) is the binding energy with (without) Coulomb potential given by Eq. (8). In order to get a comprehensive evaluation, the experimental ERE parameters for neutron-neutron are $(a_0, r_0) = (-18.5, 2.80)$ fm.

Model	V_0 (MeV)	R (fm)	c (fm)	a_0 (fm)	r_0 (fm)	$B_{\alpha\Xi^0}$ (MeV)	$B_{\alpha\Xi^-}$ (MeV)
DG	24	1.74	0.65	-4.9(-4.9)	1.9(1.9)	2.0(2.1)	3.4(3.5)
ESC08c	18	1.65	0.24	-5.7(-5.3)	2.7(2.7)	NB(NB)	0.8(0.8)
$t/a = 11$	14.5	1.83	0.38	-6.2(-6.0)	3.1(3.0)	NB(NB)	0.8(0.9)
$t/a = 12$	11.7	1.90	0.37	-7.3(-6.9)	3.7(3.7)	NB(NB)	0.5(0.5)
$t/a = 13$	6.7	2.16	0.35	-6.8(-6.6)	5.7(5.6)	NB(NB)	0.2(0.2)

ESC08c ΞN potential and first principles HAL QCD ΞN potential for the purpose of seeing whether such differences are manifest in the predictions for low energy properties. My assumptions were as follows: i. α is strongly bound and low compressible particle. ii. The mass gap between ΞN and $\Lambda\Lambda$ is somehow removed and treated by coupled-channel HAL QCD method. iii. Coupled-channel contribution from higher channels $\Xi N - \Lambda\Sigma - \Sigma\Sigma$ in $^{33}S_1$ is not considered. iv. $^5_{\Xi}H$ must show an explicit core- Ξ structure. v. Both α and Ξ particles are in S-wave states. vi. ΞN potential is spin- and isospin averaged potential.

$\alpha + \Xi$ potentials were obtained by using SFP model. Then the resultant $\alpha\Xi$ potentials were fitted by a Woods-Saxon type functions. The binding energies and scattering phase shift parameters were calculated by solving the Schrödinger equation using the fit potentials as input for DG, ESC08c and HAL QCD (at $t/a = 11, 12, 13$) potentials. The numerical results showed that none of the potentials support nuclear bound states for $^5_{\Xi}H$. But when attractive Coulomb interaction was taken into account, the $^5_{\Xi}H$ system become Coulomb-assisted bound state around 0.5 MeV, although it was still very shallow.

Curiously enough, the results were in agreement with estimations of Hiyama et al. [8] where they have found just Coulomb-assisted bound state around 0.57 MeV for $k_f = 0.9$ (there, the binding energies was a function of the Fermi momentum of nuclear matter, k_f) and roughly consistent with the calculation by Myint and Akaishi [6]. Myint and Akaishi asserted explicitly that the large part of 1.7 MeV binding energy is due to $\Xi^- + \alpha$ Coulomb interaction.

In conclusion, even though Nijmegen ESC08c and HAL QCD ΞN potential have significantly dissimilar isospin and spin components, my numerical results showed that both potential models lead to almost qualitatively consistent results. Namely, ${}^5_{\Xi}H$ cannot be a pure atomic or nuclear bound state, instead, it could be only a Coulomb-assisted resonance state that appears about 0.5 MeV below the threshold of $\alpha + \Xi^-$. The derived $\alpha + \Xi$ potential can be used in few-body model based on α -cluster structures of Ξ hypernuclei [10, 16].

-
- [1] H. Tamura *et al.*, Observation of a spin-flip $M1$ transition in ${}^7_{\Lambda}Li$, *Phys. Rev. Lett.* **84**, 5963 (2000).
 - [2] K. Nakazawa *et al.*, The first evidence of a deeply bound state of $\Xi^- - {}^{14}N$ system, *Prog. Theor. Phys.* **2015**, 033D02 (2015).
 - [3] S. Acharya *et al.* (A Large Ion Collider Experiment Collaboration), First observation of an attractive interaction between a proton and a cascade baryon, *Phys. Rev. Lett.* **123**, 112002 (2019).
 - [4] T. Hatsuda, K. Morita, A. Ohnishi, and K. Sasaki, $p\Xi^-$ Correlation in Relativistic Heavy Ion Collisions with Nucleon-Hyperon Interaction from Lattice QCD, *Nucl. Phys. A* **967**, 856 (2017), the 26th International Conference on Ultra-relativistic Nucleus-Nucleus Collisions: Quark Matter 2017.
 - [5] Y. Kamiya, K. Sasaki, T. Fukui, T. Hyodo, K. Morita, K. Ogata, A. Ohnishi, and T. Hatsuda, Femtosopic study of coupled-channels $N\Xi$ and $\Lambda\Lambda$ interactions, *Phys. Rev. C* **105**, 014915 (2022).
 - [6] K. S. Myint and Y. Akaishi, Double-Strangeness Five-Body System, *Prog. Theor. Phys.* **117**, 251 (1994).
 - [7] E. Hiyama, M. Kamimura, T. Motoba, T. Yamada, and Y. Yamamoto, ΛN spin-orbit splittings

- in ${}^9_{\Lambda}Be$ and ${}^{13}_{\Lambda}C$ studied with one-boson-exchange ΛN interactions, [Phys. Rev. Lett. **85**, 270 \(2000\)](#).
- [8] E. Hiyama, Y. Yamamoto, T. Motoba, T. A. Rijken, and M. Kamimura, Light Ξ hypernuclei in four-body cluster models, [Phys. Rev. C **78**, 054316 \(2008\)](#).
- [9] E. Hiyama, Y. Funaki, N. Kaiser, and W. Weise, Alpha-clustered hypernuclei and chiral SU(3) dynamics, [Prog. Theor. Phys. **2014**, 013D01 \(2014\)](#).
- [10] E. Hiyama and K. Nakazawa, Structure of $S = -2$ hypernuclei and hyperon-hyperon interactions, [Ann. Rev. Nucl. Part. Sci. **68**, 131 \(2018\)](#).
- [11] E. Hiyama *et al.*, Possible lightest Ξ hypernucleus with modern ΞN interactions, [Phys. Rev. Lett. **124**, 092501 \(2020\)](#).
- [12] H. Garcilazo, A. Valcarce, and J. Vijande, Maximal isospin few-body systems of nucleons and Ξ hyperons, [Phys. Rev. C **94**, 024002 \(2016\)](#).
- [13] H. Garcilazo, A. Valcarce, and J. Vijande, Ξ^-t quasibound state instead of $\Lambda\Lambda nn$ bound state, [Chin. Phys. C **44**, 024102 \(2020\)](#).
- [14] H. Garcilazo and A. Valcarce, $\Lambda\Lambda N - \Xi NN$ S wave resonance, [Chin. Phys. C **44**, 104104 \(2020\)](#).
- [15] F. Etminan and A. Aalimi, Examination of the $\phi - NN$ bound-state problem with lattice QCD $N - \phi$ potentials, [Phys. Rev. C **109**, 054002 \(2024\)](#).
- [16] H. Le, J. Haidenbauer, U.-G. Meißner, and A. Nogga, $A = 4 - 7$ Ξ hypernuclei based on interactions from chiral effective field theory, [Eur. Phys. J. A **57**, 1 \(2021\)](#).
- [17] K. Sasaki *et al.* (HAL QCD Collaboration), Coupled-channel approach to strangeness $S = -2$ baryon-baryon interaction in lattice QCD, [Prog. Theor. Phys. **2015**, 113B01 \(2015\)](#).
- [18] K. Sasaki *et al.* (HAL QCD Collaboration), $\Lambda\Lambda$ and $N\Xi$ interactions from lattice QCD near the physical point, [Nucl. Phys. A **998**, 121737 \(2020\)](#).
- [19] M. M. Nagels, T. A. Rijken, and J. J. de Swart, Baryon-baryon scattering in a one-boson-exchange-potential approach. II. Hyperon-nucleon scattering, [Phys. Rev. D **15**, 2547 \(1977\)](#).
- [20] T. A. Rijken and Y. Yamamoto, Extended-soft-core baryon-baryon model iii. $s = -2$ hyperon-hyperon/nucleon interaction (2006), [arXiv:nucl-th/0608074 \[nucl-th\]](#).
- [21] E. Friedman and A. Gal, Constraints on Ξ^- nuclear interactions from capture events in emulsion, [Phys. Lett. B **820**, 136555 \(2021\)](#).
- [22] M. M. Nagels, T. A. Rijken, and Y. Yamamoto, Extended-soft-core baryon-baryon ESC08

- model III. $S = -2$ hyperon-hyperon/nucleon interaction (2015), [arXiv:1504.02634 \[nucl-th\]](#).
- [23] L. Fabbietti, V. M. Sarti, and O. V. Doce, Study of the Strong Interaction Among Hadrons with Correlations at the LHC, [Annu. Rev. Nucl. Part. Sci. **71**, 377 \(2021\)](#).
- [24] S. Acharya *et al.* (ALICE Collaboration), Unveiling the strong interaction among hadrons at the LHC, [Nature **588**, 232 \(2020\)](#).
- [25] F. Etminan *et al.* (HAL QCD Collaboration), Spin-2 $N\Omega$ dibaryon from lattice QCD, [Nucl. Phys. A **928**, 89 \(2014\)](#), special Issue Dedicated to the Memory of Gerald E Brown (1926-2013).
- [26] T. Iritani *et al.*, $N\Omega$ dibaryon from lattice QCD near the physical point, [Phys. Lett. B **792**, 284 \(2019\)](#).
- [27] S. Gongyo *et al.* (HAL QCD Collaboration), Most strange dibaryon from lattice QCD, [Phys. Rev. Lett. **120**, 212001 \(2018\)](#).
- [28] N. Ishii, S. Aoki, and T. Hatsuda, Nuclear force from lattice QCD, [Phys. Rev. Lett. **99**, 022001 \(2007\)](#).
- [29] N. Ishii *et al.* (HAL QCD Collaboration), Hadron–hadron interactions from imaginary-time nambu–bethe–salpeter wave function on the lattice, [Phys. Lett. B **712**, 437 \(2012\)](#).
- [30] S. Aoki, B. Charron, T. Doi, T. Hatsuda, T. Inoue, and N. Ishii, Construction of energy-independent potentials above inelastic thresholds in quantum field theories, [Phys. Rev. D **87**, 034512 \(2013\)](#).
- [31] G. Satchler and W. Love, Folding model potentials from realistic interactions for heavy-ion scattering, [Phys. Rep. **55**, 183 \(1979\)](#).
- [32] T. Miyamoto *et al.* (HAL QCD), $\Lambda_c N$ interaction from lattice QCD and its application to Λ_c hypernuclei, [Nucl. Phys. A **971**, 113 \(2018\)](#).
- [33] F. Etminan and M. M. Firoozabadi, Simple Woods-Saxon type form for $\Omega\alpha$ and $\Xi\alpha$ interactions using folding model, [Chin. Phys. C **44**, 054106 \(2020\)](#).
- [34] C. Dover and A. Gal, Ξ Hypernuclei, [Ann. Phys. **146**, 309 \(1983\)](#).
- [35] I. Filikhin, V. Suslov, and B. Vlahovic, Bound state of the $\alpha\Lambda\Lambda\Xi$ system, [J. Phys. G Nucl. Part. Phys. **35**, 035103 \(2008\)](#).
- [36] K. Miyagawa and M. Kohno, A realistic approach to the ΞNN bound-state problem based on Faddeev equation, [Few. Body. Syst. **62**, 65 \(2021\)](#).
- [37] F. Etminan and M. R. Hadizadeh, Three-body Faddeev calculations for ${}^6_{\Lambda\Lambda}He$ and ${}^6_{\Omega\Omega}He$

- hypernuclei, *Chin. Phys. C* **46**, 104103 (2022).
- [38] F. Etminan, K. Sasaki, and T. Inoue, Coupled-channel $\Lambda_c K^+ - p D_s$ interaction in the flavor SU(3) limit of lattice QCD, *Phys. Rev. D* **109**, 074506 (2024).
- [39] Y. Akaishi, *Cluster Models and Other Topics*, International review of nuclear physics (World Scientific, 1986).